

# Analysis of Ocean Thermal Energy Conversion (OTEC) Potential using Closed-cycle System Simulation of 100 MW Capacity in Bali Sea

Ismail Ali Hajar Aswad<sup>1</sup>, Nanda Annisa Okasari Yusal<sup>2</sup>, Haryo Dwito Armono<sup>1</sup>, Purwanto<sup>2</sup>, Delyuzar Ilahude<sup>3</sup>, Liany Ayu Catherine<sup>1</sup> and Asfarur Ridwan<sup>1</sup>

<sup>1</sup>Faculty of Marine Technology, Sepuluh Nopember Institute of Technology, Surabaya, Indonesia

<sup>2</sup>Faculty of Fisheries and Marine Sciences, Diponegoro University, Semarang, Indonesia

<sup>3</sup>Marine Geological Research and Development Center, Bandung, Indonesia

Keywords: OTEC, Closed-cycle, Bali Sea.

**Abstract:** The Bali Sea is one of the body water that has OTEC potential because of its location in tropical region, thus it has high sea surface temperatures. This research was conducted to examine temperature differences to run the system and analyze the results of simulation of the closed-cycle OTEC system based on the simulation results of Uehara and Ikegami (1990) as a basic reference in the installation of plants and obtain net power produced by the cycle. The data used in this study is temperature in depth data per day during October 2008-June 2017 which downloaded from HYCOM website and vertical temperature data of CTD which is the result of P3GL survey on 21 May 2017 -3 June 2017. Data processing was done by calculating the differences in temperature of warm sea air on the surface and cold sea water at depth of 800 m by qualifying the minimum difference requirement of 20°C. The results of temperature data processing yield the difference in temperature minimum requirements of 20°C at all study area in the range of 21.895°C-24.7°C. The parameter values in the closed cycle OTEC system obtained are the warm sea water (TWS) and cold (TCS) temperatures of 28.4°C-30.36°C and 5.591°C-6.711°C; warm seawater pump power (PWS), cold seawater pump power (PCS), and working fluid pump power (PWF) of 10.9596-11.521 MW, 16.0596-16.621 MW, and 1.94-1.97 MW; and the heat transfer area in evaporator (AE), the heat transfer area in condenser (AC), and total of heat transfer area (AT) of 0.737-1.7478 x10<sup>5</sup> m<sup>2</sup>, 0.9685-1.614 x10<sup>5</sup> m<sup>2</sup>, and 1.7058-3.3435 x10<sup>5</sup> m<sup>2</sup>. Net power potential of OTEC in Bali Sea has range between 70-71 MW with maximum net power found at Point 2 of 71.041 MW with capacity of 100 MW and produce a cycle efficiency of 0.41323 or 41.323%.

## 1 INTRODUCTION

Sunlight reaches the earth's surface 35-100 m (Avery and Wu, 1994). The sea in the tropics absorbs the sun continuously all the time causing sea surface temperatures to vary to reach 27°C-29°C. The total area of the world's tropical oceans totaling 60 million km<sup>2</sup> produces energy equivalent to 250 trillion fuels per yield (Nihous, 2005). Seas in Indonesia with a total thermal potential of 2.5x10<sup>23</sup> Joules and an efficiency of 3%, can produce power of 240,000 MW (Prabowo, 2012).

Sea Heat Energy Conversion (OTEC) is one of the solutions in developing ocean energy by using temperatures between the sea and the deep sea in the

tropics to produce electrical energy with a minimum temperature difference of 20°C (Nihous, 2007). Energy generated from sea heat is very suitable to be applied in tropical regions such as Indonesia. If this can be done effectively and on a large scale, OTEC provides a renewable energy source that is needed to complement various energy problems (Syamsuddin, 2015).

Various studies and OTEC studies that have been carried out in Indonesia to date have been carried out by Sinuhaji (2015) in the North Bali Sea with the result of an increase in surface temperature between 28-31°C with a difference of 24°C; Negara and Koto (2016) in Karangkelong, North Sulawesi with a potential of 100 kW; and Syamsuddin (2015) at seven location points in Indonesia using World

Ocean Atlas 2009. Previous research on the potential of the OTEC in the Bali Sea is only theoretical and must be further discussed to obtain the expected results.

The goal of this research is to obtain minimum temperature difference requirement of 20°C at seven study points in the Bali Sea Waters, to obtain minimum temperature difference requirement of 20°C at seven study points in the Bali Sea Waters and to analyze the result of OTEC system simulation closed cycle with 100MW power capacity.

## 2 SEA WATER TEMPERATURE AND OTEC OVERVIEW

### 2.1 Vertical Distribution of Sea Water Temperature

Solar thermal energy is absorbed by the surface layer and penetrates the deeper sea. However, the conduction process occurs so slowly that only a small portion of the heat flowing in (Santos et al., 2012). The temperature will decrease dramatically at depths between 200-300 m to 1000 m. This decreasing depth layer is known as a thermocline that is thinner at low latitudes than at high latitudes. At a depth of 300-1000 m, seawater does not change in temperature and ranges from 0-3°C. It is influenced by cold temperatures originating from the mass of water from the poles then flowing into the equatorial region (Santos et al., 2012) equatorial region (Santos et al., 2012).

### 2.2 Ocean Thermal Energy Conversion (OTEC)

It is a powerplant by utilizing the temperature difference of seawater on the surface and the temperature of the seawater where the ocean, which covers two-thirds of the earth's surface area, receives heat from solar radiation. This thermal energy can be utilized by converting it into electrical energy with a technology called Ocean Thermal Energy Conversion (OTEC). A large amount of energy is absorbed by the oceans in the form of heat that comes from the sun's rays and magma located beneath the seabed (Masutani and Takahashi, 2001).

### 2.3 OTEC System

The OTEC system is divided into three types, namely open cycle, closed cycle, and hybrid cycle

(Aldale, 2017). The closed-cycle OTEC system is more widely studied than other systems based on various source literature. A closed-cycle requires a turbine that is smaller than an open cycle (open-cycle) and can increase the efficiency of the electrical energy produced by the generator (Masutani and Takahashi, 2001). This study will use a closed-cycle OTEC system.

## 2.4 OTEC Power Calculation

The power generated from the turbine generator in the OTEC system according to (Uehara and Ikegami, 1990) is

$$P_G = m_{WF} \eta_T \eta_G (h_1 - h_2) \quad (1)$$

Where

- $P_G$  : turbine generator power (MW)
- $m_{WF}$  : the mass flow rate of the working fluid (kg/s)
- $\eta_T$  : turbine efficiency = 0.85
- $\eta_G$  : generator efficiency
- $h_1 - h_2$  : a decrease in adiabatic heat between the evaporator and the condenser

The net electrical power equation used is

$$P_N = P_G - (P_{WS} + P_{CS} + P_{WF}) \quad (2)$$

Where

- $P_N$  : clean electric power (MW)
- $P_G$  : turbine generator power (MW)
- $P_{WS}$  : warm sea flow pump power (MW)
- $P_{CS}$  : cold sea water pump power (MW)
- $P_{WF}$  : working fluid pump power (MW)

## 3 METHOD

The method used in this research is a quantitative method. The first step is taking CTD temperature data and collecting HYCOM temperature data by using a data model downloaded from the website <http://ncss.hycom.Org/thredds/catalog.html> with the Net Common Data File (NetCDF) format which used daily temperature data for 9 years (October 2008-June 2017) with a resolution of 1/12° and a depth of 0-5500 m. The second step is the processing of CTD temperature data and HYCOM temperature data processing by using data verification using the Root Mean Square Error (RMSE) (Neill and Hashemi, 2018).

$$RMSE = \sqrt{\frac{1}{n} \sum_{i=1}^n (s_i - o_i)^2} \quad (3)$$

Where

n : number of observation

O : observation value

Si : predictive value

Formula parameters to determine the bias values by Neill and Hashemi (2018), as follows:

$$bias = \bar{s} - \bar{o} \quad (4)$$

### 3.1 Calculation of Sea Water Pump Power and Working Fluid

To calculate sea water pump power and working fluid is used the formulation by Uehara and Ikegami (1990) and it can be followed this step.

The power of warm seawater pump is calculated by the formulation as follows

$$P_{WS} = \frac{m_{WS} \Delta H_{WS} g}{\eta_{WSP}} \quad (5)$$

Cold sea water pump power is calculated with the following formulation:

$$P_{CS} = \frac{m_{CS} \Delta H_{CS} g}{\eta_{CSP}} \quad (6)$$

Power of the working fluid pump is calculated by the formulation as follows:

$$P_{WF} = \frac{m_{WF} \Delta H_{WF} g}{\eta_{WFP}} \quad (7)$$

Where

$P_{WS}$  : warm sea flow pump power (MW)

$P_{CS}$  : Cold sea water pump power (MW)

$P_{WF}$  : working fluid pump power (MW)

$m_{WS}$  : Mass flow rate of warm sea water (t/s)

$m_{CS}$  : Cold sea water mass flow rate (t/s)

$m_{WF}$  : Working fluid mass flow rate (t/s)

$\eta_{WSP}$  : Warm water pump efficiency

$\eta_{CSP}$  : Cold water pump efficiency

$\eta_{WFP}$  : Efficiency of the working fluid pump

$\Delta H_{WS}$  : The total pressure difference in Warm water pipes

$\Delta H_{CS}$  : The total pressure difference in the Cold water pipe

$\Delta H_{WF}$  : The total pressure difference in the working fluid pipe

g : acceleration of gravity (m/s<sup>2</sup>)

### 3.2 Calculation of Sea Water Pump Power and Working Fluid

In this study, the  $A_T$  value was obtained from the interpolation between the temperature difference value ( $\Delta T$ ) from the temperature data processing and the AT value using Uehara and Ikegami (1990).

To determine the total heat transfer area, the following equation can be used from Uehara and Ikegami (1990):

$$A_T = A_E + A_C \quad (8)$$

On the evaporator, the heat transfer area is calculated by the formula:

$$A_E = \frac{Q_E}{U_E (\Delta T_m)_E} \quad (9)$$

To find out the value of the heat transfer rate on the evaporator, can use the formula:

$$Q_E = m_{WF} (h_1 - h_4) \quad (10)$$

In the condenser, the heat transfer area is calculated by the formula:

$$A_C = \frac{Q_C}{U_C (\Delta T_m)_C} \quad (11)$$

To find out the value of the heat transfer rate in the condenser, can use the formula:

$$Q_C = m_{WF} (h_2 - h_3) \quad (12)$$

Where

$A_T$  : The area of heat transfer in the evaporator (m<sup>2</sup>)

$A_E$  : The area of heat transfer in the condenser (m<sup>2</sup>)

$A_C$  : Total heat transfer area (m<sup>2</sup>)

$Q_E$  : Heat transfer rate to the evaporator

$Q_C$  : Heat transfer rate to the condenser

$(\Delta T_m)_E$  : logarithmic mean temperature differences (LTMD) pada evaporator

$(\Delta T_m)_C$  : logarithmic mean temperature differences (LTMD) pada kondensor

$(h_1 - h_4)$  and  $(h_2 - h_3)$  : the enthalpy value matches the Rankine cycle

### 3.3 Calculation of OTEC Net Power and Rankine Cycle Efficiency

The net power of OTEC ( $P_{NET}$ ) can be calculated using equation (2). The efficiency of the Rankine cycle ( $\eta_{Ran}$ ) can be calculated by the equation

$$\eta_{Ran} = \frac{P_G}{Q_E} \quad (13)$$

Where

$\eta_{Rankine}$  : Rankine cycle efficiency

$P_G$  : Turbine generator power (MW)

$Q_E$  : Heat transfer rate to the evaporator

## 4 RESULT AND DISCUSSION

### 4.1 Verification of HYCOM and CTD Temperature Data

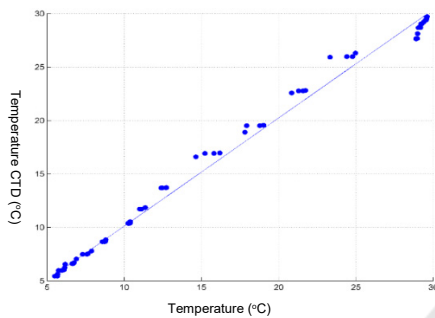


Figure 1: Distribution of Temperature Value to Depth between HYCOM Data and CTD Data (Source: Data Processing).

The error value obtained and the data distribution graph below, then HYCOM has good data and is considered capable of representing the temperature conditions of the CTD collection.

### 4.2 Vertical Temperature Distribution in the Bali Sea

The temperature of warm seawater at the surface ( $T_{WS}$ ) and the temperature of cold seawater at depth ( $T_{CS}$ ) are obtain to get the difference in temperature ( $\Delta T$ ) between sea level and depth.

In general, temperatures that tend to be uniform in the mixed layer (Figure 2-8) are caused by the turbulence mechanism by wind and waves and heat flux at sea level. Changes in temperature at the surface of the sea and layers are mixed due to the strength of the wind influenced by monsoons so that the temperature at the surface of the sea and the layers are mixed experiencing monthly variations. Also, according to Atmadipoera and Hasanah (2017), the temperature in the mixed layer shows seasonal variability. The cause of this variability is thought to be due to the influence of the mass movement of water in the Java Sea and the Flores Sea which partly entered the Lombok Strait.

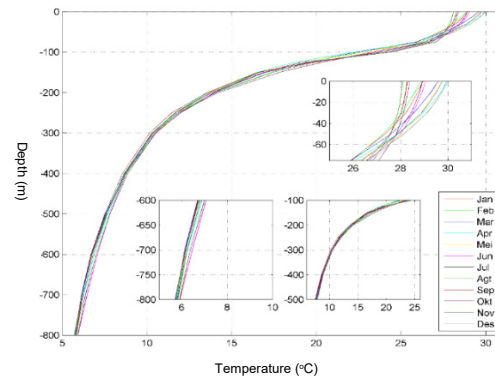


Figure 2: Temperature Vertical Distribution Plot of 2008 - 2017 at Point 1 (Source: Data Processing).

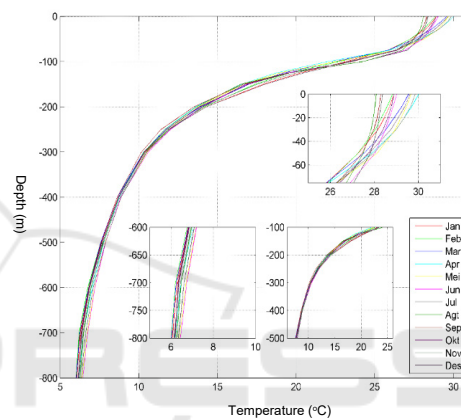


Figure 3: Temperature Vertical Distribution Plot of 2008 - 2017 at Point 2 (Source: Data Processing).

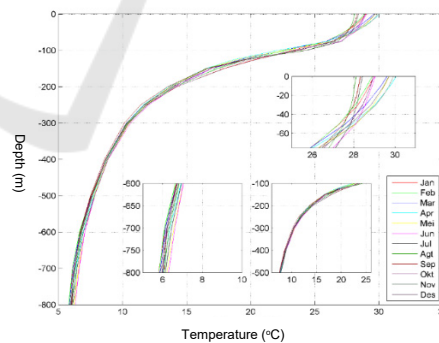


Figure 4: Temperature Vertical Distribution Plot of 2008 - 2017 at Point 3 (Source: Data Processing).

### 4.3 Difference in Surface and Depth Temperature in the Bali Sea

From 2008 to 2017, the maximum temperature difference value occurs in April at all points as shown in Figure 12 with the average maximum temperature difference of 23,998°C. From April to

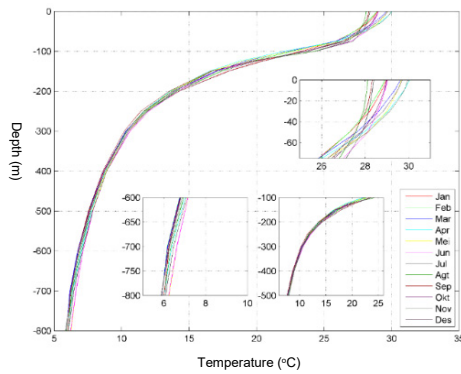


Figure 5: Temperature Vertical Distribution Plot of 2008 - 2017 at Point 4 (Source: Data Processing).

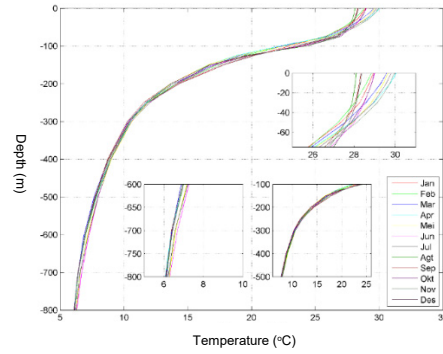


Figure 8: Temperature Vertical Distribution Plot of 2008 - 2017 at Point 7 (Source: Data Processing).

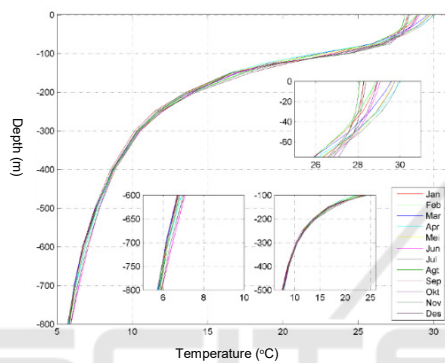


Figure 6: Temperature Vertical Distribution Plot of 2008 - 2017 at Point 5 (Source: Data Processing).

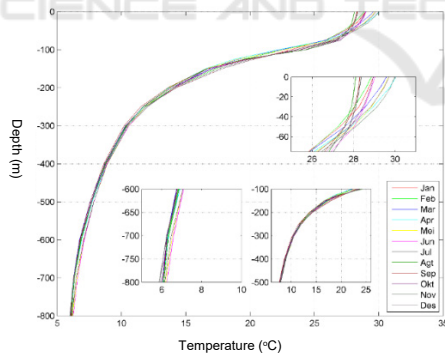


Figure 7: Temperature Vertical Distribution Plot of 2008 - 2017 at Point 6 (Source: Data Processing).

August, the temperature difference decreased quite dramatically at all points with an average decrease of 1,975°C. The lowest temperature difference occurred in August, with an average of 22,023°C. Then, starting in August there was a significant increase of 1,933°C at all points until November with an average temperature difference of 23,956°C for the month.

Bali Sea meets the potential OTEC requirements of more than 20°C during October 2008-2017 with a temperature difference ranging from 21.9°C to 24.5°C. However, this potential needs to be studied further to get the true potential by determining the net power value based on a closed-cycle system simulation of 100 MW.

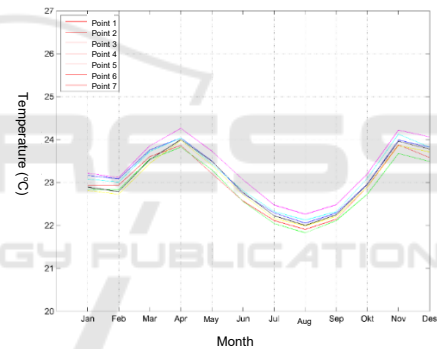


Figure 9: Average Monthly Temperature Difference in 2008-2017. (Source: Data Processing).

## 4.4 Closed Cycle System Simulation

### 4.4.1 Warm and Cold Water Temperature Profiles

This shows that the temperature of cold seawater is not affected by monsoons like warm seawater temperatures. The almost uniform temperature is caused by a large enough density in the deep sea so that the mass of seawater is denser. The high density is caused by layers in the deep sea not having a direct influence from the wind, the intensity of sunlight, precipitation and evaporation, and cloud cover such as the temperature of warm seawater.

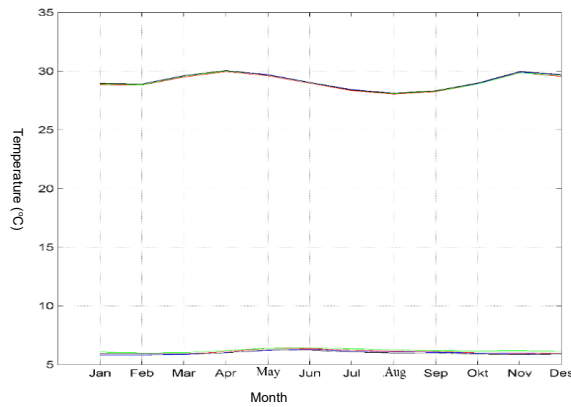


Figure 10: Variations in Surface Temperature Monthly ( $T_w$ ) and Temperature Depth ( $T_c$ ) in 2008-2017 (Source: Data Processing).

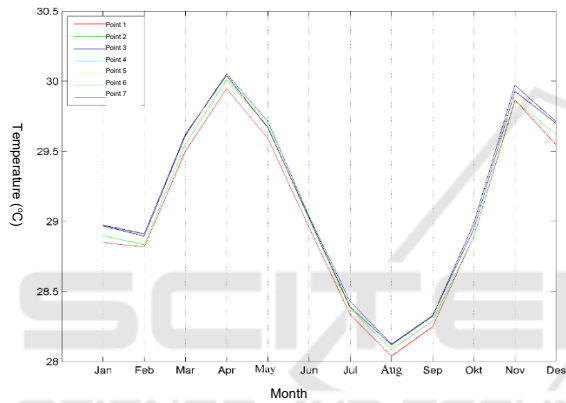


Figure 11: Monthly Variations of Warm Sea Water Temperature on  $T_{wS}$  2008-2017. (Source: Data Processing).

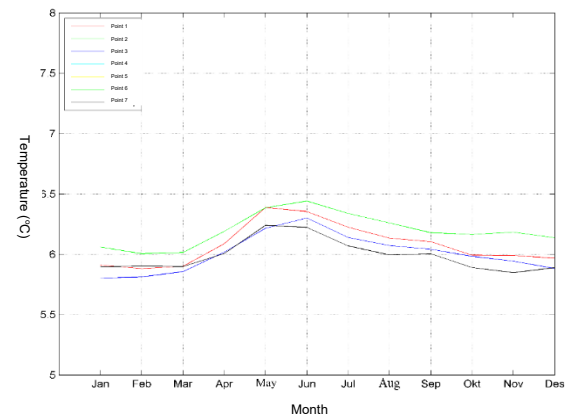


Figure 12: Monthly Variations in Cold Sea Water Temperature at Depths of 800 m ( $T_c$ ) in 2008-2017 (Source: Data Processing).

#### 4.4.2 Pump Power for Warm Water, Cold Water and Working Fluid

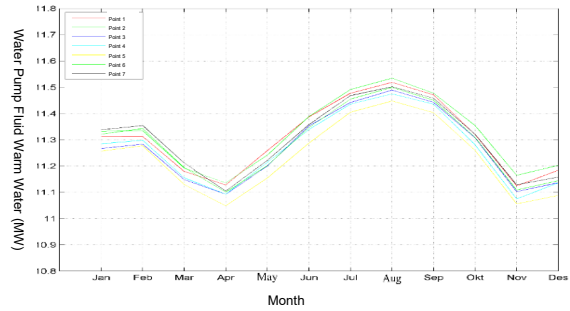


Figure 13: Monthly Warm Water Pump Power ( $P_{ws}$ ) in 2008-2017 (Source: Data Processing).

Warm seawater pump power reached the highest rate in August, which was an average of 11,495 MW. Meanwhile, the lowest warm seawater pump power occurred in April with an average value of 11.1 MW.

Coldwater pump power reached the highest rate in August, which was an average of 16,595 MW. Meanwhile, the lowest warm seawater pump power occurred in April with an average value of 16.2 MW. Coldwater pump power is stable from year to year with a range between 1.94-1.97 MW.

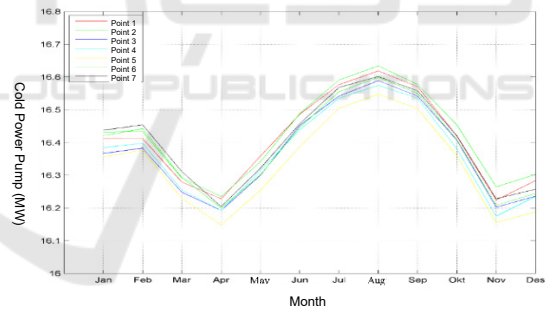


Figure 14: Monthly Cold Power Pump ( $P_{cs}$ ) 2008-2017 (Source: Data Processing).

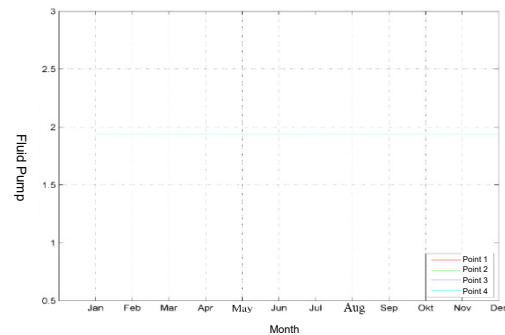


Figure 15: Power of Monthly Working Fluid Pump ( $P_{wf}$ ) in 2008-2017 (Source: Data Processing).

### 4.4.3 Heat Transfer Area

The heat transfer area in the evaporator reached the highest number in August, which was an average of  $1.70164 \times 10^5 \text{ m}^2$ . Meanwhile, the lowest heat transfer area in the evaporator occurred in April with an average value of  $0.99052 \times 10^5 \text{ m}^2$ .

The area of heat transfer in the condenser reached the highest number in August, namely an average of  $1,58466 \times 10^5 \text{ m}^2$  and the lowest in April with an average value of  $1.130330 \times 10^5 \text{ m}^2$ .

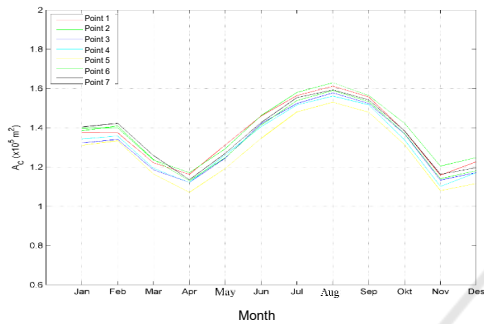


Figure 16: Area of Heat Transfer in Monthly Evaporators 2008-2017 (Source: Data Processing).

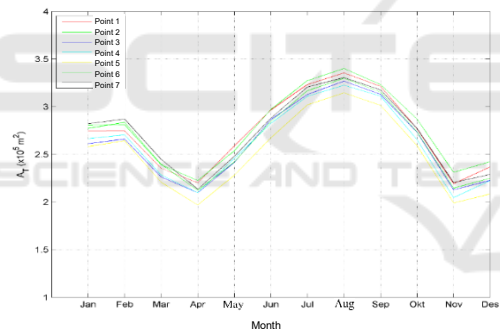


Figure 17: Heat Transfer in Monthly Condenser ( $A_c$ ) 2008-2017 (Source: Data Processing).

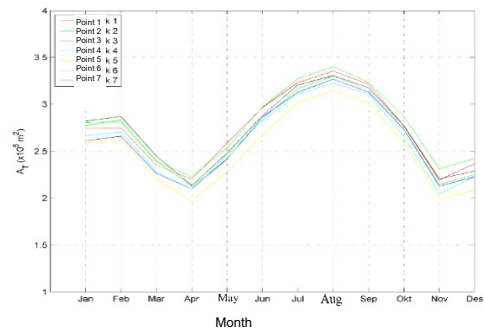


Figure 18: Total Heat Transfer Area ( $A_T$ ) in 2008 -2017 (Source: Data Processing).

### 4.5 Calculation of OTEC Net Power and Cycle Efficiency

The results of the OTEC net power estimation results are listed in the table 1.

The highest net power for 9 years (Table 1.) was achieved in April with an average net power of 70,759 MW and the lowest occurred in August with an average net power of 69,969 MW. The maximum cycle efficiency is 0.4061 at Point 5. The highest cycle efficiency occurs in April with an average maximum value of 0.402, while the lowest cycle efficiency occurs in August with an average minimum value of 0.3704.

Table 1: OTEC Clean Power at Study Point 2008-2017.

Location	Temperature Difference ( $^{\circ}\text{C}$ )	Clean Power (MW)		
		Average	Min	Max
Point 1	22.969	70.348	69.922	70.711
Point 2	22.896	70.318	69.891	70.689
Point 3	23.140	70.416	69.981	70.775
Point 4	23.157	70.423	70.010	70.810
Point 5	23.327	70.491	70.064	70.863
Point 6	23.053	70.381	69.961	70.759
Point 7	22.990	70.356	69.956	70.750

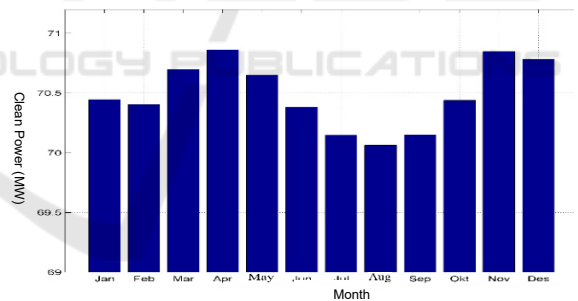


Figure 19: Monthly Net Power in 2008-2017 at the Potential Point (Source: Data Processing).

Table 2: Efficiency of the Rankine Cycle at the Study Point in 2008-2017.

Location	Clean Power Average (MW)	Efficiency		
		Average	Min	Max
Point 1	70.348	0.3855	0.3685	0.4000
Point 2	70.318	0.3843	0.3672	0.3992
Point 3	70.416	0.3882	0.3709	0.3026
Point 4	70.423	0.3885	0.3720	0.4040
Point 5	70.491	0.3912	0.3742	0.4061
Point 6	70.381	0.3868	0.3700	0.4020
Point 7	70.356	0.3858	0.3698	0.4016

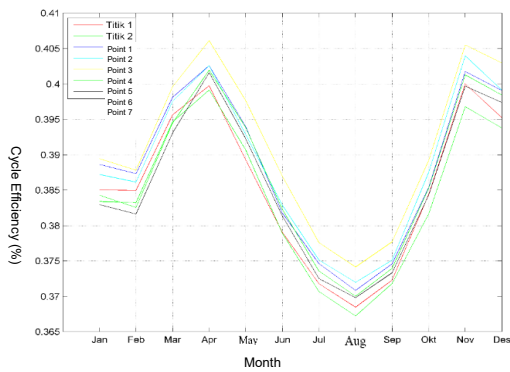


Figure 20: Efficiency of Monthly Cycles in 2008-2017 (Source: Data Processing).

### 4.6 Discussion of Closed Cycle OTEC System Simulation

The power of warm seawater pumps ( $P_{WS}$ ) and cold seawater pump power ( $P_{CS}$ ) decreases but is not very significant, while the power of the working fluid pump ( $P_{WF}$ ) is stable against the increase in  $T_{WS}$ . Meanwhile, the net power ( $P_{NET}$ ) increased from 70.06 MW to 70.86 MW.  $P_{NET}$  value is derived from the remaining power generated by the turbine due to be used to pump warm seawater, cold seawater, and working fluid.

The heat transfer area in the evaporator ( $A_E$ ) decreases from  $1.61633 \times 10^5 \text{m}^2$  to  $0.89701 \times 10^5 \text{m}^2$ . Likewise, the area of heat transfer in the condenser ( $A_C$ ) which also decreased from  $1.53015 \times 10^5 \text{m}^2$  to  $1.0705882 \times 10^5 \text{m}^2$ . This decrease certainly affects the value of the area of heat transfer on the condenser ( $A_T$ ) which decreased from  $3.14648 \times 10^5 \text{m}^2$  to  $1.967596 \times 10^5 \text{m}^2$ .

Table 3: Simulation Parameter Value Based on 100 MW Closed Cycle Simulation.

Location	Pump Power (MW)			Heat Transfer Area ( $\times 10^5 \text{m}^2$ )			Net Power (MW)	Cycle Efficiency (%)
	$P_{WS}$	$P_{CS}$	$P_{WF}$	$A_E$	$A_C$	$A_T$		
Point 1	11.306	16.406	1.94	1.361	1.367	2.728	70.348	0.3855
Point 2	11.321	16.421	1.941	1.387	1.384	2.771	70.318	0.3843
Point 3	11.272	16.372	1.951	1.300	1.328	2.628	70.416	0.3882
Point 4	11.269	16.369	1.951	1.293	1.324	2.617	70.423	0.3885
Point 5	11.235	16.335	1.94	1.232	1.285	2.517	70.491	0.3912
Point 6	11.289	16.389	1.951	1.331	1.348	2.679	70.381	0.3868
Point 7	11.302	16.402	1.95	1.354	1.362	2.716	70.256	0.3858

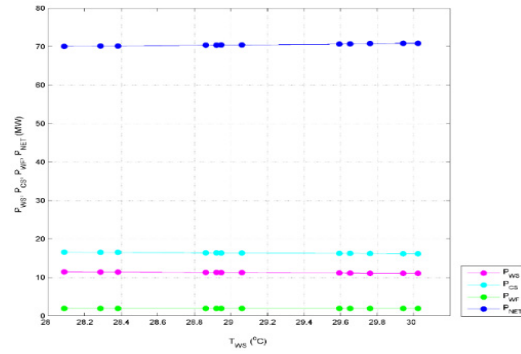


Figure 21: Relationship Between Pump Power ( $P_{WS}$ ,  $P_{CS}$ ,  $P_{WF}$ ) and Clean Power ( $P_{NET}$ ) (Source: Data Processing).

Uehara and Ikegami (1990) stated that the cost of the heat exchanger is one of the components that most cuts the cost of generation, around 25-50% of the total cost. Therefore, it is necessary to obtain the minimum objective function value by increasing the production of clean electric power and the heat exchanger needed to optimize the area of heat transfer can be suppressed.

The graph (Figure 24.) shows a linear relationship between net power and cycle efficiency. Increasing the value of net power will also increase the value of cycle efficiency. To produce a maximum electric power of 70.86 MW, the efficiency of the issued Rankine cycle reaches a maximum of 0.4061 or 40.61%. The efficiency of the Rankine cycle comes from how efficient the OTEC generator is in releasing power to pump warm seawater ( $P_{WS}$ ), cold seawater ( $P_{CS}$ ), and working fluid ( $P_{WF}$ ). Thus, the greater the net power produced, the pump power produced must also be greater and this will increase the value of the Rankine cycle efficiency.

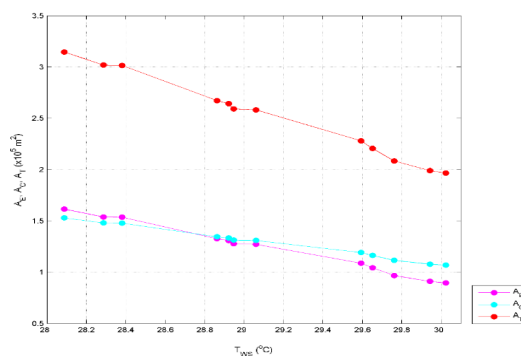


Figure 22: Relationship Between Heat Transfer Area in Evaporator and Condenser ( $A_E$ ,  $A_C$ ) and Total Heat Transfer Area ( $A_T$ ) (Source: Data Processing).

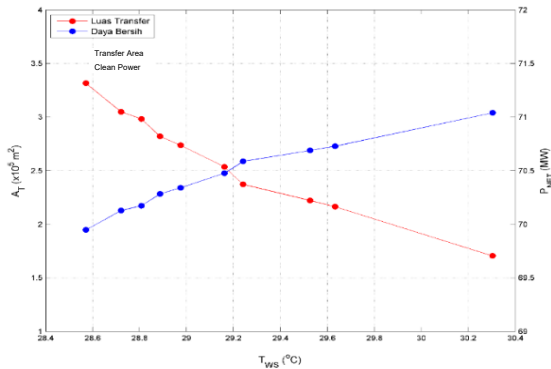


Figure 23: Relationship Between Total Heat Transfer Area ( $A_T$ ) and Clean Electricity Power ( $P_{NET}$ ) (Source: Data Processing).

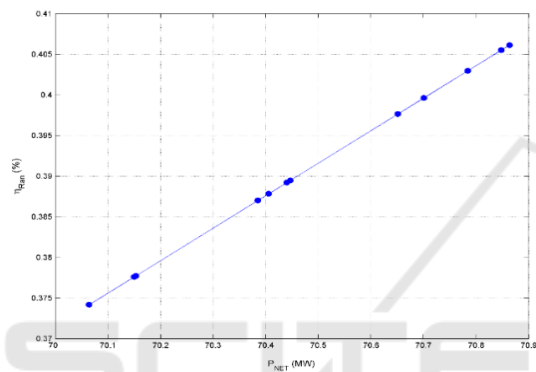


Figure 24: Relationship Between Clean Electric Power ( $P_{NET}$ ) and Cycle Efficiency ( $\eta_{Ran}$ ) (Source: Data Processing).

## 5 CONCLUSION

1. Minimum temperature difference requirement of 20°C at seven study points in the Bali Sea Waters was fulfilled during 2008-2017 with a range between 21.9°C - 25.3°C.
2. Potential net electric power OTEC in the Bali Sea has a range between 69.8-70.8 MW with a maximum net power found at Point 5 of 70.86 MW with a capacity of 100 MW with cycle efficiency of 0.4061 or 40.61%.
3. Based on the simulation of closed cycle OTEC, the components that describe and support the potential of OTEC are warm sea water temperature ( $T_{WS}$ ) and cold water ( $T_{CS}$ ) of 28°C-30°C and 5.7°C-6.4°C; warm sea water pump power ( $P_{WS}$ ), cold sea water pump power ( $P_{CS}$ ), and working fluid pump power ( $P_{WF}$ ) of 11,048-11,543 MW, 16,148-16,634 MW, and 1.94-1.97 MW; heat transfer area on the evaporator ( $A_E$ ), heat transfer area on the condenser ( $A_C$ ), and the

total heat transfer area ( $A_T$ ) of 0,897-1,772x10<sup>5</sup> m<sup>2</sup>, 1,07059-1,62968x10<sup>5</sup> m<sup>2</sup>, and 1,9676-3.401794x10<sup>5</sup> m<sup>2</sup>.

## REFERENCES

- Aldale, Abdullah Mohammed. 2017. "Open Access Ocean Thermal Energy Conversion (OTEC) American Journal of Engineering Research (AJER)." (4):164–67.
- Avery, W.H. and Chih Wu. 1994. *Renewable Energy from The Ocean: A Guide To OTEC*. Oxford University Press, Inc., New York, 446 p.
- Masutani, and Takahashi. 2001. "Ocean Thermal Energy Conversion (Otec)." 1(1997):1993–99.
- Negara, Ridho Bela dan J. Koto. 2016. Potential of 100 kW of Ocean Thermal Energy Conversion in Karangkelong, Sulawesi Utara, Indonesia. *International Journal of Environmental Research & Clean Energy*, 5 (1): 1-10
- Neill, Simon P., Hashemi, M. Reza. 2018. *Fundamentals of Ocean Renewable Energy: Chapter 8-Ocean Modelling for Resource Characterization*. Academic Press. Elsevier 1<sup>st</sup> Edition
- Nihous, Gérard C. 2007. "A Preliminary Assessment of Ocean Thermal Energy Conversion Resources." *Journal of Energy Resources Technology, Transactions of the ASME* 129(1):10–17.
- Prabowo, H. 2012. *Atlas Potensi Energi Laut*. J. M&E, 10(4): 65-71.
- Santos, Fran, Moncho Gómez-Gesteira, Maite deCastro, and Inés Álvarez. 2012. "Variability of Coastal and Ocean Water Temperature in the Upper 700 m along the Western Iberian Peninsula from 1975 to 2006." *PLoS ONE* 7(12):2–8.
- Sinuhaji, A.R. 2015. Potential Ocean Thermal Energy Conversion (OTEC) in Bali. *KnE Energy*, 1: 5-12.
- Syamsuddin, Mega L., Adli Attamimi, Angga P. Nugraha, and Syahrir Gibran. 2015. "OTEC Potential in The Indonesian Seas." *Energy Procedia* 65:215–22.
- Uehara, Haruo dan Yasuyuki Ikegami. 1990. Optimization of a Closed Cycle OTEC System. *Journal of Solar Energy Engineering*, 112: 247-256.